

The ground state of clean and defected graphene: Coulomb interactions of massless Dirac fermions, pair-distribution functions and spin-polarized phases.

M.W.C. Dharma-wardana*
National Research Council of Canada,
Ottawa, Canada. K1A 0R6

(Dated: 29 June 2006)

First-principles density functional calculations for graphene and defected graphene are used to examine when the quasi-2D electrons near the Fermi energy in graphene could be represented by massless fermions obeying a Dirac-Weyl (DW) equation. The DW model is found to be inapplicable to defected graphene containing even $\sim 3\%$ vacancies or N substitution. However, the DW model holds in the presence of weakly adsorbed molecular layers. The possibility of spin-polarized phases (SPP) of DW-massless fermions in pure graphene is considered. The exchange energy is evaluated from the analytic pair-distribution functions as well as in k -space. The kinetic energy enhancement of the spin-polarized phase nearly cancels the exchange enhancement, and the correlation energy plays a dominant residual role. The correlation energies are estimated via a model four-component 2D electron fluid whose Coulomb coupling matches that of graphene. While SPPs appear with exchange only, the inclusion of correlations suppresses them in ideal graphene.

PACS numbers: PACS Numbers: 71.10.Lp, 75.70.Ak, 73.22-f

I. INTRODUCTION.

Graphene and related materials (e.g, nanotubes, fullerenes) have become a mine of novel technologies and new horizons in physics[1]. These include cosmological models on honeycomb branes, superconductivity on bipartite lattices[3], nanotubes[4, 5], Hubbard models[6], spin-phase transitions[7], nanostructures[8] and other aspects of strongly correlated electrons[9]. The carbon atoms in graphene form a quasi-two-dimensional (Q2D) honeycomb lattice and contribute one electron per carbon to form an unusual 2D electron system (2DES) with a massless Fermions obeying a Dirac-Weyl (DW) equation near the Fermi points[10, 11, 12]. The hexagonal Brillouin zone has two inequivalent points $\mathbf{K}=(1/3, 1/\sqrt{3})$ and $\mathbf{K}'=(-1/3, 1/\sqrt{3})$, in units of $2\pi/a_0$, where a_0 is the lattice constant. The simplest tight-binding model with nearest-neighbour hopping t is sufficient to describe the valence and conduction bands (π and π^*) near the \mathbf{K} , \mathbf{K}' points, i.e, at the Fermi energy E_F , where the bandgap is zero. The Dirac-Weyl 2D electron system (DW-2DES) is nominally “half-filled”, with the π^* band unoccupied, (see Fig. 1) and has spin and valley degeneracies, with a Berry phase associated with the valley index[12].

The above picture assumes a perfect 2-D sheet of C atoms in a honeycomb lattice held in place by the σ -bonding structure of the C framework. In practice, since defects are favoured by the entropy term in the free energy, some carbon atoms may be missing, forming vacancies; they may also be substituted with other defect atoms. The surface itself may be covered with adsorbed gases. Hence the nature of the density of states (DOS)

near the Fermi energy in systems with vacancies and substituted atoms needs to be considered[13, 14]. Removing a carbon atom effectively removes four valence electrons from the system, and the resulting vacancy may or may not lead to a magnetic, conducting or insulating ground state. Replacing a C atom by, say, a nitrogen atom provides five valence electrons. We find that at typical concentrations of 3% or more, the Dirac-Weyl picture fails, and the Fermi energy moves into a bandgap or to regions with a high density of states. However, if less extreme situations are considered (e.g, adsorbed gases on graphene), the DW picture is found to hold true.

The Fermi liquid found in metals and semi-conductor interfaces is characterized by the Wigner-Seitz radius r_s of the sphere (or disk in 2D) which contains one electron. When expressed in atomic units (involving the effective mass m^* of the electrons), r_s becomes the ratio of the potential energy to the kinetic energy, i.e, a measure of *the strength of the Coulomb interaction*. Hence $r_s < 1$ provides a regime where Fermi-liquid perturbation theory is strictly valid. The vanishing of the density of states and the effective mass of the electrons in DW-2DES near the Fermi points implies that the strict Fermi-liquid picture breaks down in perfect graphene.

The DW-2DES can be doped to contain carrier electrons (in the π^* band), or holes as well (in the π band), and provides a rich system which retains the massless-fermion character, as long as the material is not strongly modified. However, electron-electron interactions in the DW-2DES may modify the π and π^* bands, lift the sublattice (valley) degeneracies, or stabilize spin-polarized phases (SPP) in preference to the unpolarized state, if the doping level or the strength of the Coulomb interaction could be varied. The effect of electron-electron interactions has been most extensively studied in Fermi-liquid-like electron systems found in GaAs/AlAs inter-

*Email address: chandre.dharma-wardana@nrc.ca

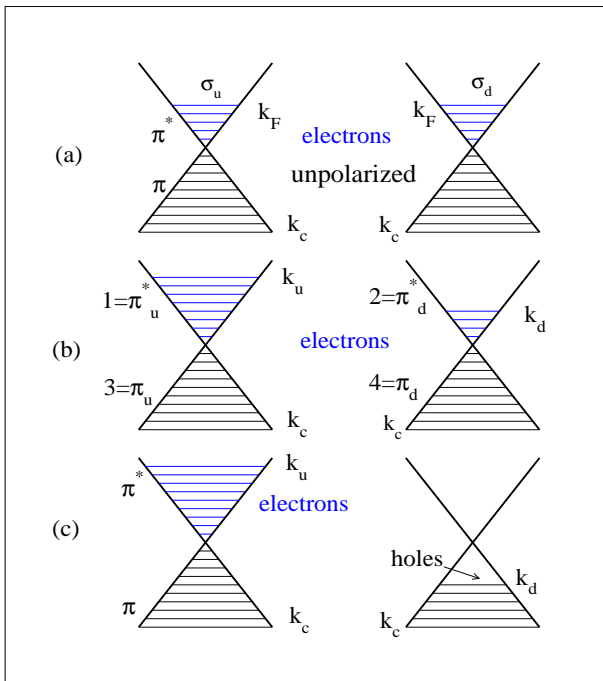


FIG. 1: (Color online) Linear dispersion bands near a \mathbf{K} point where the π^* and π bands cross. In (a) we show a doped unpolarized system with equal occupation of the up-spin (σ_u) and down-spin states. In (b) the polarized system has only electron carriers. In (c) both electron and hole carriers occur. This is the only possibility for spin polarization if doping is zero ($k_F = 0$ and $k_u = k_d$).

faces or Si/SiO₂-inversion layers. The SPP in such GaAs/AlAs-based 2DES, predicted to appear at low coupling ($r_s \sim 2 - 4$) if perturbation methods are used, get pushed to high coupling ($r_s \sim 26$) if non-perturbative theory (NPT) were used[16, 17]. The two-valley 2DES does *not* show a SPP in NPT, unlike for one-valley systems, presumably because of the preponderance of the (three times as many) direct Coulomb interactions over the exchange interactions[18]. The exchange and correlation energy E_{xc} in the 4-component Si/SiO₂ electron system were calculated in Ref.18 using the classical-map hyper-netted-chain (CHNC) technique, accurately recovering the Quantum Monte-Carlo (QMC) results in every coupling regimes[19]. CHNC provides the pair-distribution functions (PDFs) g_{ij} as a function of the coupling strength. Then E_{xc} is evaluated via a coupling constant integration, providing a fully non-local, transparent approach. The method has been successfully applied to the 2DES[20], 3DES[21], the 2-valley 2DES in SiO₂ interfaces[18], the thick quasi-2DES in HIGFETS[22], and the electron-proton system[23]. However, the full non-local treatment of exchange and correlation in graphene involves an 8×8 matrix of two-component PDFs because of the spin, and valley indices as well as the presence of π, π^* bands. Hence in this study we first consider the exchange energies via an an-

alytic evaluation of the non-interacting PDFs. The correlation energies are estimated by appealing to our results for the spin-polarized four-component two-valley 2-D electron system (2v-2DES) of Si-MOSFETS. The non-interacting PDFs of the DW-2DES, $\mathcal{G}_{ij}^0(r)$ involve two components, the first being a Bessel function as in the ordinary 2DES, while a second, associated with the cosine of the angle of e-e scattering, involves products of Bessel and Struve functions. The exchange energy enhancement of the spin-polarized phase nearly cancels the kinetic energy enhancement, implying that the correlation energy plays the dominant residual role. We find that while there are stable SPPs in an exchange-only approach, including the correlation energy using the 2v-2DES data stabilizes the graphene-2DES in the unpolarized state. This conclusion is not surprising since the Coulomb coupling strength in graphene is $\sim 2-3$, and no SSFS are found in electron liquids at such low coupling, except as artifacts of low-order theories.

In the following section we present first-principles calculations for pure graphene, graphene with $\sim 3\%$, and $\sim 12\%$ vacancy concentrations, and show that the DW-model is inapplicable to such systems. We also consider systems with N-substitution as the lattice distortion effects are smaller here. Nevertheless, even here the DW-model does not seem to be applicable. However, if we consider a graphene layer having a metastable sheath of N₂ molecules adsorbed on it, with no disruption of the σ -bonding network, the DW-model does remain applicable. Thus, having established the limits of the DW-model, we proceed to examine the exchange and correlation effects among DW-fermions, and show that a stable spin phase transition is found only in “exchange only” models which neglect electron correlation effects.

II. DENSITY-FUNCTIONAL CALCULATIONS OF GRAPHENE SYSTEMS

Simple tight-binding models(TBM) can be trusted only if they are validated by more detailed calculations and experiments. While TBM can be successfully exploited within a limited energy window for pure graphene, the effect of vacancies and lattice substituents etc., needs detailed consideration. A vacancy removes 4 valence electrons, distorts the bond lengths and angles around the vacancy, creating pentagonal networks and compensating larger networks, localizing electrons near the vacancy and changing the structure of the electronic density of states (DOS). The bond-lengths and the network structure is better preserved with N substitution. Here an extra electron is added to the graphene system for every N substitution. Attempting to treat such effects using tight-binding methods augmented by, say, T -matrix theory etc., to account for impurity effects are well known to be strongly model dependent. Nevertheless, some insight has already been gained from short-ranged scatterer models where lattice relaxation and

other very important issues are not handled[31, 32, 33] However, density-functional theory (DFT) has an excellent track record in just such problems where electronic and ionic energy minimization can be carried out until the Hellman-Feynman forces on atoms around the vacancy or the substituant are reduced to zero. There are a number of such DFT calculations already in the literature[13, 14], mainly concerned with energetics and bonding. Here we examine the bands and DOS of these systems, with an eye on the limits of validity of the DW-2DES model.

We have used the Vienna *ab initio* simulation package (VASP)[25] which implements a spin-density functional periodic plane-wave basis calculation. The projected augmented wave (PAW) pseudopotentials[25] have been used for C and N. The C pseudopotential has already been used in several graphene-type calculations (e.g., Ref. 13). The N pseudopotential was also further tested by a study of the N₂ dimer where an equilibrium bond distance of 1.11 Angstroms was obtained, in good agreement with other DFT calculations as well as results from detailed configuration interaction studies etc.[26], where a value of 1.095 Å is reached. The $\sim 3\%$ and $\sim 12\%$ vacancy calculations were done with 32-atom and 8-atom graphene-like unit cells. These systems are thus *not* truly disordered, but provide reference densities of states which acquire smearing when some disorder is introduced by sampling other configurations using larger simulation cells[27]. When vacancies are introduced into graphene, the large stresses are relieved by the neighbours (C-atoms near the vacancy) moving towards the vacancy. The distortion persists to at least the third neighbours, and generates a bond-length distribution varying from about 1.398Å to 1.45 Å. If the vacancies are replaced by N substitution, the structural distortions are smaller but the changes in the DOS can be equally drastic, as we show below.

Yuchen Ma et al.[13] have found that N₂ molecules may form a metastable layer near carbon nanotubes and graphene. Iyakutti et al[27] have also found similar stabilization, where the N₂ layer is less stable than if it were at infinity, but held in place by an energy barrier. Although this is a 'weakly adsorbed' state, the interaction energy between the graphene layer and the N₂ layer is about as strong as between two graphene sheets. Hence we have looked at the band-structure and DOS of such a fully N₂ covered graphene sheet as well. Here the Dirac-Weyl behaviour is preserved. In Fig. 2 we show the band structure of pure graphene (top panel), and also a graphene sheet with a layer of N₂ molecules, with each N₂ aligned on every Kékulé-bond position (bottom panel). The sheet of N₂ molecules is positioned about 3Å above the graphene sheet. The interaction energy per carbon (or per N) is about 0.2 eV. The regime of DW linear dispersion around the **K** point is reduced from that of pure graphene. This is in contrast to the interaction between two graphene sheets, where the bands near the **K**-point become parabolic[15].

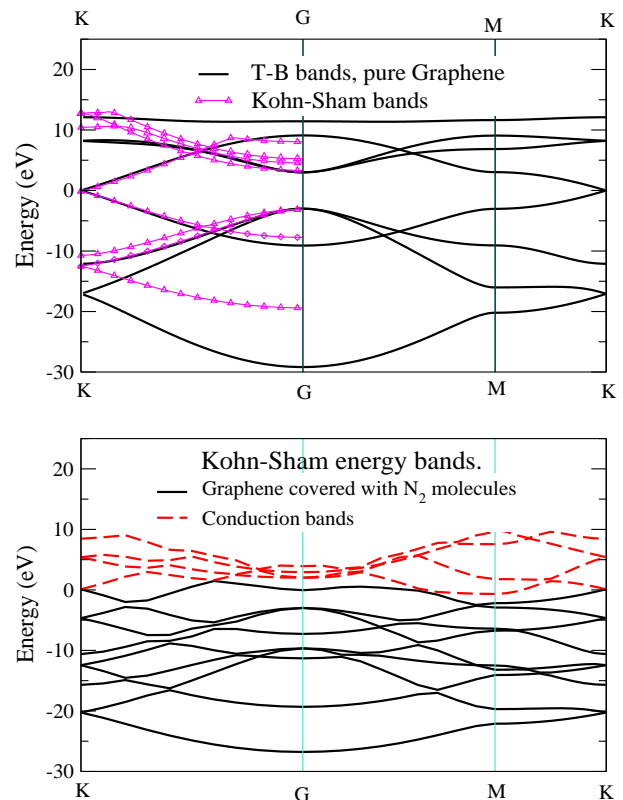


FIG. 2: (Color online) Band structure of pure graphene (top panel), and that of fully N₂ covered graphene. The Fermi energy is at $E+F=0$. Conduction bands are shown in red. The bands obtained from a standard sp^3 tight-binding scheme are compared with the DFT bands for graphene in the top panel.

However, when vacancies or N atoms are introduced into the graphene network at relatively significant concentrations (e.g., 3%-12 %), the DOS modifies and shifts to produce a large density of states near the Fermi energy E_F . This is shown in the top panel of Fig. 3. The calculation is for an ordered system with 1/8 or 1/32 alloying of vacancies or N, and may be used as reference points for a consideration of a disordered system. The calculations used exchange-correlation functionals based on the Ceperley-Alder type[29], and no spin polarized states are expected for a conductive system with an enhanced DOS, as seen in the figure. On the other hand, the existence of such an enhanced DOS near E_F in graphene with 12% vacancies, would be of importance to possible superconductivity of these systems.

The electronic density of states for a lower density vacancy system, i.e., with one vacancy per 32 carbon atoms, is shown in the lower panel. Here the system *acquires a gap* near E_F , and the material is an insulator. If the vacancy concentration is further decreased, we expect the energy gap to slowly decrease and recover the Dirac-Weyl model in the limit of pure graphene. But, as seen from the DOS at 12% vacancies, we see that as the vacancy concentration is increased from 3%, the en-

ergy gap closes and E_F positions to a high-DOS region. Meanwhile, an energy gap opens about 1 eV below the Fermi energy. Thus we see that a *vacancy induced metal-insulator transition* is possible (see however, Ref. 30). This picture becomes considerably less sharp if the vacancies are not considered to form a periodic array. In any case, our conclusion that the Dirac-Weyl model is inapplicable even at 3% vacancy concentrations probably remains valid. The observations of the quantum Hall effect and other signatures of the DW model clearly indicate that good low-vacancy regions of graphene foils are the subject of these experiments. Another aspect of low-density vacancies or substituents in graphene is the issue of spin-polarized ground states. The reported results depend on the size and edge structure of finite sheet fragments[14], or the possibility of further C-atom adsorption on N-substituted sites[13]. The calculations are sensitive to the treatment of exchange and correlation, as in first-principles theories of magnetism in transition-metal oxides. Hence a reliable discussion of magnetism in graphene-like systems would require an assessment of Coulomb interactions in Dirac-Weyl electrons. Hence we revert to the main object of the present study, viz., the nature of exchange and correlation effects in pure graphene.

III. THE 2DES IN GRAPHENE NEAR THE FERMI POINTS.

The band structure of graphene near the \mathbf{K} points, i.e., close to the Fermi energy, are displayed in Fig. 2. The kinetic energy near the \mathbf{K} points is given by a Dirac-Weyl Hamiltonian of the form:

$$H_k = V_F(p_x\tau_z\sigma_x + p_y\sigma_y) \quad (1)$$

Here $\tau_z = \pm 1$ defines the degenerate valleys, and σ_x, σ_y denote the x and y Pauli matrices that act in the space of the two atoms in each unit cell. The π, π^* bands of spin and valley degenerate states (Fig. 1) show a linear dispersion $E = \pm V_F \hbar k$. This form requires a cutoff momentum K_c such that the number of states in the Brillouin zone is conserved. That is, if A_0 is the area per carbon, then

$$K_c^2 = 4\pi(1/A_0) \quad (2)$$

The electron density N_c at half-filling is $1/A_0$, with $A_0 = a_0^2\sqrt{3}/2$, since one π electron of arbitrary spin is provided by each carbon atom. The Fermi velocity $V_F = ta_0\sqrt{3}/2$ is thus the slope of the linear dispersion, with $V_F \sim 5.5 \text{ eV}\text{\AA}$. If the DW-2DES is embedded in a medium with dielectric constant ϵ_0 , then we define

$$g^0 = \frac{e^2/\epsilon_0}{\hbar V_F} = \frac{e^2}{\epsilon_0 a_0} / (t\sqrt{3}/2). \quad (3)$$

This is the ratio of a typical Coulomb energy to the hopping energy and hence is usually taken as the Coulomb coupling constant of the DW-2DES. This ratio plays the

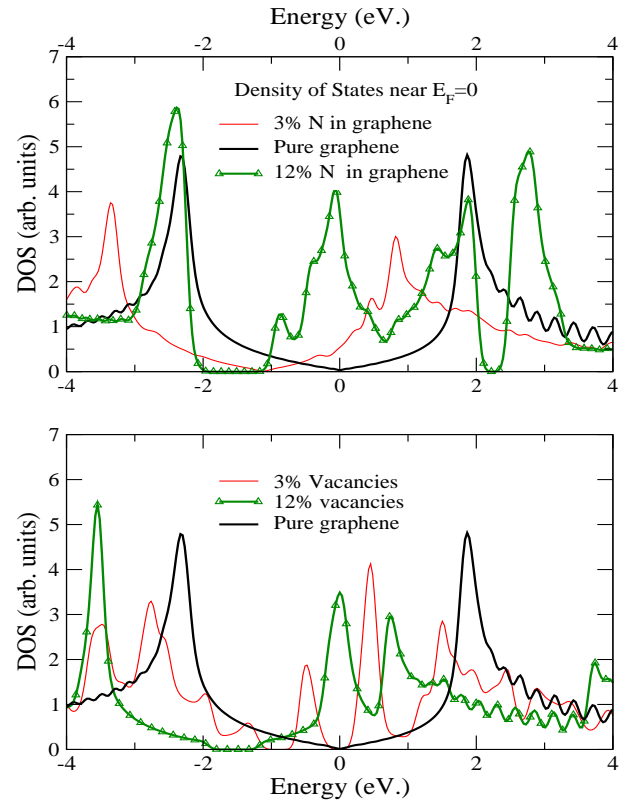


FIG. 3: (Color online) DOS of pure graphene compared with $\sim 3\%$ and $\sim 12\%$ concentrations of substituted N atoms (top panel), calculated using a periodic substitution model. The Fermi energy is set to zero. Bottom panel shows the effect of $\sim 3\%$, 12% vacancies in graphene.

same role as the r_s parameter in electron-gas theory of nonrelativistic finite-mass fermions, and is a measure of the strength of the Coulomb interaction. The usual r_s is not available for DW-2DES since the effective mass m^* is zero and there is no effective Bohr radius. The coupling constant g^0 is *maximized* if ϵ_0 is unity, and consistent with this case we assume $g^0 = 2.7$, $V_F = 5.39 \text{ eV}\text{\AA}$, with $e^2/\epsilon_0 = 14.4$, for our DW-2DES studies.

The 4-component-eigenfunction envelopes of the kinetic energy term are made up of two-component functions $U = (b, e^{i\phi_k})$, $U' = (e^{i\phi_k}, b)$ and $O = (0, 0)$ where ϕ_k is the angle of the vector \vec{k} in the 2-D plane. Thus

$$F_{b,\vec{k}}^{\mathbf{K}}(r) = (2A)^{1/2}(U, O)_T \chi_\sigma \quad (4)$$

$$F_{b,\vec{k}}^{\mathbf{K}'}(r) = (2A)^{1/2}(O, U')_T \chi_\sigma \quad (5)$$

Here $b = \pm 1$ is a π^*, π band index, $(\dots)_T$ indicates the transpose, and χ_σ is the spin function. Then, using $v = 1, 2$ as a valley index, the Coulomb interaction term in

the Hamiltonian may be written in the form:

$$\begin{aligned}
H_I = & \frac{1}{8A} \sum_{v_i, b_i, \sigma_i} \sum_{\mathbf{k}, \mathbf{p}, \mathbf{q}} V_q \left[b_1 b_4 e^{i\{\phi^*(\mathbf{k}) - \phi(\mathbf{k}+\mathbf{q})\}} + 1 \right] \\
& \times \left[b_2 b_3 e^{i\{\phi^*(\mathbf{p}) - \phi(\mathbf{p}+\mathbf{q})\}} + 1 \right] \times \\
& a_{\mathbf{k}, v_1, b_1, \sigma_1}^+ a_{\mathbf{p}+\mathbf{q}, v_2, b_2, \sigma_2}^+ a_{\mathbf{p}, v_2, b_3, \sigma_2} a_{\mathbf{k}+\mathbf{q}, v_1, b_4, \sigma_2} \quad (6)
\end{aligned}$$

Here a^+, a are electron creation and annihilation operators and $V_q = 2\pi e^2 / (\epsilon_0 q)$ is the 2D Coulomb interaction. The phase factors introduce a novel $\cos(\theta)$ contribution where θ is the scattering angle, not found in the usual jellium-2DES. The resulting form of the exchange energy per Carbon is:

$$\begin{aligned}
E_x/E_u = & -\frac{A_0 g^0/k_c}{(2\pi)^2} \frac{1}{4} \sum_{b_1, b_2, \sigma} \int_0^{2\pi} d\theta dk dp \quad (7) \\
& \times kp \frac{1 + b_1 b_2 \cos(\theta)}{|\mathbf{k} - \mathbf{p}|} n_{b_1, \sigma}(k) n_{b_2, \sigma}(p)
\end{aligned}$$

In the above we have included the intrinsic coupling constant g^0 and the energy unit $E_u = V_F k_c$ in the expressions. Here $k_c = K_c/\sqrt{2} = \sqrt{(4\pi n_c)}$ is based on the electron density per spin species, $n_c = N_c/2 = 1/(2A_0)$. The above form of the exchange energy can be reduced to an evaluation of a few elliptic integrals[7]. The normal ‘‘half-filled’’ DW-2DES can be doped with electrons or holes; but it is easy to show that symmetry enables us to limit to one type of doping. However, given a system, with an areal density of N_δ dopant electrons per valley, with $n_\delta = N_\delta/2$ per spin, the carriers in the spin-polarized system could be electrons only, or both electrons and holes, as shown in Fig. 1 for the π^* and π bands at one \mathbf{K} point. The intrinsic system with $n_\delta = 0$ can be an unpolarized state, or spin-polarized state with electrons and holes. Such *purely exchange driven* systems have been studied by Peres et al.[7], while the correlations effects have not been considered. Here we evaluate the exchange energy E_x from the non-interacting PDFs, and include the correlation energy E_c estimated from the 2v-2DES with the same coupling strength ($r_s = g^0$) and spin-polarization.

A. Electron Pair-distribution functions of the Dirac-Weyl 2DES

Although we are dealing with an intrinsically four-component system (2-valleys, 2-spin states), as seen from Fig. 1, we need to consider the redistribution of electrons and holes among the π^* and π bands when comparing the energy of spin-polarized states with the corresponding unpolarized state. The exchange energy is a consequence of the anti-symmetry of the Slater determinant made up of non-interacting eigenfunctions. Thus only the non-interacting PDFs are needed to calculate the exchange energy. They are also the spring-board for calculating the interacting PDFs via the CHNC method.

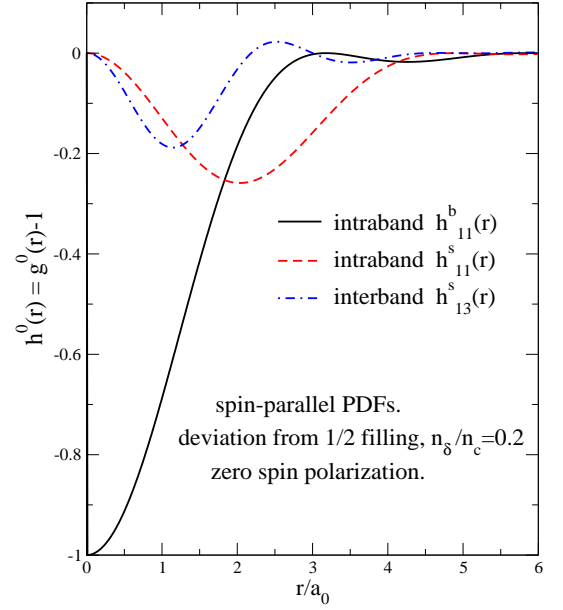


FIG. 4: (Color online) The Bessel-like and Struve-like non-interacting, parallel-spin PCFs $h^b(r)$ and $h^s(r)$ for the unpolarized doped system. The bands are numbers as in Fig. 1(b). The anti-parallel non-interacting PCFs are zero. The lattice constant $a_0 = 2.47\text{\AA}$.

From Fig. 1 we see that the e-e interactions at a given valley can be constructed from (i) interactions with a $\pi^* \sigma_u$ band of up-spin electrons of density n_u , filled to k_u , (ii) a $\pi^* \sigma_d$ set of electrons or a $\pi \sigma_d$ spin-down holes, of density n_d , filled up to k_d (iii) the $\pi \sigma_u$ band, with electron density n_c , filled to k_c , and (iv) the $\pi \sigma_d$ band, density n_c , filled to k_c . There will also be similar intervalley terms. Each term in this 4×4 matrix, denoted by $\mathcal{G}_{ij}(r)$ where $i, j = 1 \dots 4$, will have two components associated with those in U' and $U = (b, e^{i\phi_k})$. Thus $\mathcal{G}_{ij}(r) = g_{ij}^b(r), g_{ij}^s(r)$, where the superfixes ‘b, s’ indicate that the noninteracting forms are Bessel-function like, and Struve-function like, respectively. These components will be denoted by a superfix $c = b, s$. The Struve form arises from the $\cos(\theta)$ terms in the Coulomb interaction. The numbering scheme of the matrix is shown in Fig. 1(b). We denote the pair-correlation functions (PCFs) $\mathcal{H}_{ij}(r) = \mathcal{G}_{ij}(r) - 1$, or the components by $h_{ij}^c(r) = g_{ij}^c(r) - 1$. The non-interacting forms are indicated by a superscript zero. Thus we have:

$$\begin{aligned}
h_{ij}^{0,b}(r) &= -(n_i n_j)^{-1} \int_0^{k_i} \frac{d\mathbf{k}_1}{(2\pi)^2} \int_0^{k_j} \frac{d\mathbf{k}_2}{(2\pi)^2} e^{i(\mathbf{k}_1 - \mathbf{k}_2) \cdot \mathbf{r}} \\
&= -\frac{2}{k_i r} J_1(k_i r) \frac{2}{k_j r} J_1(k_j r) \quad (8) \\
h_{ij}^{0,s}(r) &= -(n_i n_j)^{-1} \int_0^{k_i} \frac{d\mathbf{k}_1}{(2\pi)^2} \int_0^{k_j} \frac{d\mathbf{k}_2}{(2\pi)^2} \\
&\quad \cos(\theta_1 - \theta_2) e^{i(\mathbf{k}_1 - \mathbf{k}_2) \cdot \mathbf{r}} \\
&= -\frac{\pi}{k_i r} \frac{\pi}{k_j r} [J_0 H_1 - J_1 H_0]_i [J_0 H_1 - H_0 J_1]_j
\end{aligned}$$

Here J_0, J_1 are Bessel functions, while H_0 and H_1 are Struve H -functions. Also, in $[J_0H_1 - J_1H_0]_i$ the functions are evaluated at the argument $k_i r$. That is,

$$[J_0H_1 - J_1H_0]_i = J_0(rk_i)H_1(rk_i) - J_1(rk_i)H_0(rk_i) \quad (9)$$

The wavevectors $k_i = \sqrt{(4\pi n_i)}$ for each component i , of density n_i . We show typical noninteracting PCFs for a doped, unpolarized case as in, Fig. 1(a), with the doping fraction $n_\delta/n_c = 0.2$. In CHNC, the exchange-hole is mapped *exactly* into a classical Coulomb fluid using the Lado procedure[21]. The figure shows that the exchange-hole is strongly reduced by the presence of the $\cos(\theta)$ term which has been averaged into the Struve-like PCFs $h^s(r)$. When the Coulomb interaction is included, the $\cos(\theta)$ term has a similar mitigating effect and exchange-correlation in the DW-2DES is considerably weaker than in the corresponding 2-valley 2DES. The CHNC calculation for the 2v-2DES for the conditions stipulated in Fig. 4 show that the correlation energy is only about a third of the exchange energy. This motivates our use of the 2v-2DES for the correlation energy, while the E_x is exactly evaluated.

B. The kinetic and exchange energies.

When the doping per valley is $N_\delta = 2n_\delta$, the total number of electrons per valley is $N_t = N_c + N_\delta$. Also, using the $i = 1, 2, 3, 4$ notation of Fig. 1(b), we set $n_1 = n_u$, $n_2 = n_d$, $n_3 = n_4 = n_c$. Hence the spin polarization $s = n_u - b_d n_d$, where the band index $b_d = -1$ for holes. The degree of spin-polarization $\zeta = s/N_t$. The composition fractions, inclusive of the valley index $v=1,2$ are $x_{vi} = n_i/2N_t$. We note that $k_F = \sqrt{(2\pi n_\delta)}$, $k_u = \sqrt{\{2\pi(n_\delta + s)\}}$, $k_d = \sqrt{\{2\pi[n_\delta - s]\}}$. The exchange energy $E_x(n_\delta, \zeta)$ can be written as:

$$E_x(n_\delta, \zeta)/N_t = (N_t/2) \int \frac{2\pi r dr}{r} \quad (10)$$

$$\times \sum_{ij} x_{vi} x_{vj} [\mathcal{G}_{v,v,ij}^0(r) - 1]$$

It is understood that the Struve-like component in $\mathcal{G}_{v,v,ij}$ where v labels the valleys, is summed with the appropriate $b_i b_j$ band \pm factors. Only a sum over the components in one valley is needed in evaluating the exchange. The above formula can be made more explicit, by introducing the $b_i b_j$ band \pm factors in each case. Thus the total kinetic and exchange energy $E_{kx} = \text{K.E} + E_x$, for the case (b) of Fig. 1 can be written in terms of n_F, n_u, n_d and n_c as in Eq. 10, or in terms of k_F, k_u, k_d, k_c and A_0 as:

$$E_{kx}(\zeta) = \frac{A_0}{6\pi} \hbar V_F (k_u^3 + k_d^3) - \quad (11)$$

$$\frac{A_0}{(2\pi)^2} (g^0 \hbar V_F / 4) (\pi/2) [k_u^4 \mathcal{H}_{11}(r) + k_d^4 \mathcal{H}_{22}(r) + 2k_c^2 \{k_u^2 \mathcal{H}_{13}(r) + k_d^2 \mathcal{H}_{14}(r)\}]$$

The kinetic and exchange energy, $E_{tx}(\zeta = 0)$, of the unpolarized system, shown in Fig. 1(a), is obtained by setting $k_F = 0$ in Eq. 11. The exchange energy for the case involving *both* electron and hole carriers, Fig. 1(c) is given by a small change in Eq. 11, where the last term changes sign and becomes $-k_d^2 \mathcal{H}_{14}(r)$. If this is simplified and written using elliptic integrals, as in Ref. 7, the *change* in the exchange energy for electron and hole carriers, compared to the unpolarized case becomes

$$E_x(\zeta) = E_x(n_\delta, \zeta = 0) + \Delta E_x(\zeta) \quad (12)$$

$$\Delta E_x(\zeta) = \frac{A_0}{(2\pi)^2} (g^0/4) (E_u/k_c) [(k_u^3 + k_d^3 - 2k_F^3) R_1(1) + 2k_c k_u^2 R_2(k_u/k_c) - 2k_c k_d^2 R_2(k_d/k_c) - 4k_c k_F^2 R_2(k_F/k_c)] \quad (13)$$

As before, $E_u = \hbar V_F k_c$ is the unit of energy. For completeness, we note that

$$E_x(n_\delta = 0, \zeta = 0) = -\frac{A_0}{(2\pi)^2} (g^0/2) E_u k_c^2 R_1(1) \quad (14)$$

$$R_1(1) = 3.776 \quad (15)$$

Here the energy is per carbon atom and we have used the notation $R_1(x), R_2(x)$ for the elliptic integrals as given in Ref. 7, and taken the opportunity to correct a few typographical errors in their Eq. (15). The energy difference which determines the competition between the unpolarized and polarized phases, i.e., $\Delta E_{kx}(\zeta)$, includes the kinetic-energy corrections as well as the change in the exchange energy. It is plotted in Fig. 5. We have done the calculations in r -space using the PDFS, and in k -space via elliptic integrals, to provide independent numerical checks. Fig. 5 shows that stable spin-polarized phases appear in electron-carrier systems, if kinetic and exchange energies are used in the total energy. A noteworthy feature of Fig. 5 is the strong cancellation of the kinetic energy by the exchange energy, leading to net energies which are about 1% of the energy scale $E_u = V_F k_c$. Thus the stage is set for the phase stabilities to be determined by the correlation energies which are left out in Fig. 5.

IV. CALCULATIONS INCLUDING THE CORRELATION ENERGY.

A rigorous calculation of the correlation energy requires the self-consistent evaluation of 8×8 matrix of pair-distribution functions for many values of the coupling constant $0 \leq \lambda \leq 1$ in the interaction λ/r , and an integration over the coupling constant λ .

Although this can be envisaged within the CHNC approach, it still remains a very arduous task. Even when all the inherent symmetries in the problem are taken into account, some two-dozen PDFs need to be evaluated. Instead we outline a simplified scheme where we use the results for the correlation energy of the two-valley, two-spin (i.e., 4 component) jellium 2DES to reconstruct the

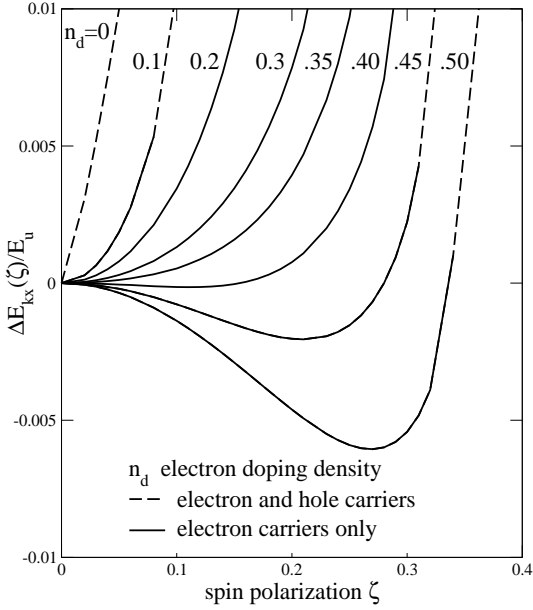


FIG. 5: (Color online) Upper panel- the energy difference ΔE_{kx} , i.e., K.E+exchange, between the polarized and unpolarized phases, in units of $E_u = V_F k_c$, as a function of the spin polarization ζ and the dopent density n_d . Electron-carrier systems, Fig. 1(b) are more stable than electron-hole systems, and show stable spin-polarized states. However, addition of the correlation energy (see Fig. 6) makes the unpolarized state the most stable phase.

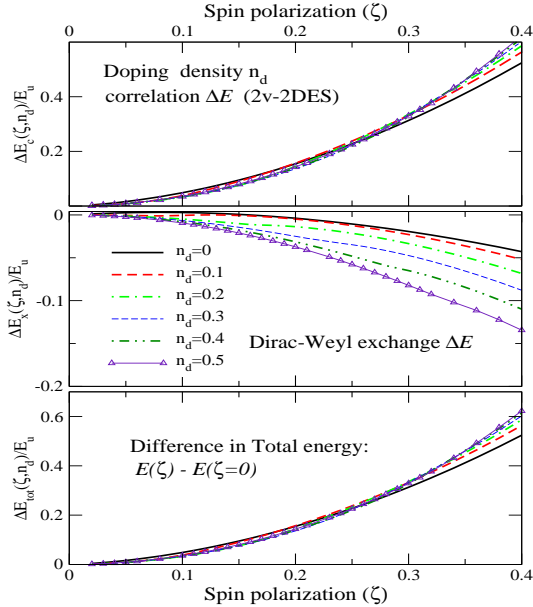


FIG. 6: (Color online) Upper panel- The correlation-energy difference $\Delta E_c(n_d, \zeta)$, i.e., between the polarized and unpolarized phases, in units of $E_u = V_F k_c$, as a function of the spin polarization ζ and the dopent density n_d . The lower panel shows the total energy difference between the polarized and unpolarized phases. The unpolarized state is the most stable phase.

correlation energy of the DW-2DES for equivalent values of the ratio of the Coulomb interaction and the kinetic energy, as discussed below. The method we use here provides a different, possibly more transparent approach than that given in a previous discussion[34]. The conclusions from the two methods are in agreement.

When the electron density of the jellium 2v-2DES is changed, the r_s value changes. In contrast, when the electron density (or, equivalently, the number of electrons per carbon) in the DW-2DES of perfect graphene is changed, the coupling constant g^0 remains unchanged. Hence the correlation energy per carbon for a doping situation involving a total of n_T electrons per carbon, at a spin-polarization ζ might be approximated by $n_T \epsilon_c^{2v}(r_s, \zeta)$, with $r_s = g^0$, where $\epsilon_c^{2v}(r_s, \zeta)$ is the corresponding 2v-2DES correlation energy. However, this result is in terms of an effective atomic unit E_{au} , intrinsic to the jellium-2DES, such that the Fermi energy $E_F = E_{cu}/r_s^2$. Since we identify the coupling constant g^0 to be r_s , the effective atomic unit $E_{au} = E_F r_s^2$. A full evaluation of the 4-component jellium 2DES from the interacting PDFs has been carried out and the correlation energy is given in parametrized form in Eq. 5 of Ref. 18. In transferring from the 2v-2DES to the DW-2DES we note that e^2/ϵ_0 which is unity in 2v-2DES becomes $g^0 V_F$ in the DW-2DES. The correlation energy enhancement is:

$$\Delta E_c(n_d, \zeta) = E_c(n_d, \zeta) - E_c(n_d, 0) \quad (16)$$

The correlation energies in jellium-2DES are evaluated from PDFs whose non-interacting forms are Bessel-type PDFs, where as the DW-2DES contain only about 1/2 the number of Bessel-type PDFs, while the other are Struve-type PDFs which bringing in a minor contribution. Thus an upper bound would be to use the estimate of $\Delta E_c(n_d, \zeta)$ given above, while a lower-bound would be about 1/2 the above estimate. The ΔE_c calculated from the jellium 4-component system using the above scheme is shown in Fig. 6. The total energy difference inclusive of the kinetic energy, E_x , and the estimated E_c , between the polarized and unpolarized phases is shown in in the lower panel of Fig. 6. Since the kinetic-energy enhancement of the polarized phase is compensated by the exchange enhancement, the total energy enhancement is determined by the correlation effects. Thus we see that the inclusion of the correlation energy suppresses the spin-polarized phase found in the exchange-only calculation.

In this work we have kept the Coulomb coupling fixed at $g^0 = 2.7$ typical of graphene, unlike in other studies[6, 7] where the coupling strength g is taken as a tunable parameter, in the spirit of Hubbard-model studies. If dielectric screening is taken into account[35], the coupling is reduced and many-body effects become smaller. We do not see a practical experimental scheme for increasing the value of the Coulomb coupling strength g^0 beyond 2.7 in the graphene system.

Even in the one-valley 2DES, the SPP of low-order theories is pushed to $g \sim 26 - 27$. In the 2v-2DES, direct terms predominate over exchange interactions, and the

SPP is not found in CHNC[18] or QMC[19] calculations. We see that the inclusion of correlations within a reasonable scheme suppresses the exchange-driven SPP in the

graphene-2DES as well. This result is in agreement with the conclusions of Ref. 34.

-
- [1] A. Geim, *Physics Today*, Jan (2005)
- [2] K. S. Novoselov et al., *Nature* **438**, 197 (2005); Y. B. Zhang et al., *Nature (London)*, **438**, 201 (2005)
- [3] J. Nagamatsu et al. *Nature(London)* **410**, 63 (2001)
- [4] N. Tit and M. W. C. Dharma-wardana, *Europhys. Lett.*, **62**, 405 (2003) J. Gonzalez, *Phys. Rev. Lett.* **88**, 76403 (2002).
- [5] C. D. Spataru, S. Ismail-Beigi, L. X. Benedict, S. G. Louie, *Phys. Rev. Lett.* **92**, 077402 (2004)
- [6] S. Sorella and E. Tosatti, *Europhys. Lett.* **19**, 699 (1996); N. M. R. Peres, M. N. A. Araújo and D. Bozi, *Phys. Rev. B* **70**, 195122 (2004)
- [7] N. M. R. Peres, F. Guinea and A. H. Castro Neto, *Phys. Rev.* **72** 174406 (2005)
- [8] J. M. Pereira Jr., V. Mlinar, F. M. Peeters, and P. Vasilopoulos, *Phys. Rev. B* **74**, 045424 (2006)
- [9] D. V. Khveshchenko, *Phys. Rev. B* **74**, 161402 (2006)
- [10] P.R. Wallace, *Phys. Rev.* **71**, 622 (1947); G. Semenov, *Phys. Rev. Lett.* **53**, 2449 (1984);
- [11] D. P. DiVincenzo and E. J. Mele, *Phys. Rev. B* **29**, 1685 (1984)
- [12] for a recent review, see T. Ando, *J. Phys. Soc. Jpn.* **74**, 777 (2005)
- [13] Yuchen Ma, A. S. Foster, A. V. Krashennnikov, and R. M. Nieminen, *Phys. Rev. B* **72**, 205416 (2005); B. I. Daln-Bo, *J. Phys. B: At. Mol. Phys.* **29**, 4907 (1996)
- [14] Hosik Lee, Young-Woo Son, Noejung Park, Seungwu Han, and Jejun Yu, *Phys. Rev. B* **72** 174431 (2005)
- [15] B. Partoens and F. Peeters, *Phys. Rev. B* **74**, 075404 (2006)
- [16] C. Attacalite et al, *Phys. Rev. Lett.* **88**, 256601 (2002)
- [17] M. W. C. Dharma-wardana and F. Perrot., *Phys. Rev. Lett.* **90**, 136601 (2003)
- [18] M. W. C. Dharma-wardana and F. Perrot, *Phys. Rev. B* **70**, 035308 (2004)
- [19] S. Conti and G. Senatore, *Europhys. Lett.* **36**, 695, (1996)
- [20] François Perrot and M. W. C. Dharma-wardana, *Phys. Rev. Lett.* **87**, 206404 (2001)
- [21] M. W. C. Dharma-wardana and F. Perrot, *Phys. Rev. Lett.* **84**, 959 (2000)
- [22] M. W. C. Dharma-wardana, *Phys. Rev. B* **72**, 125339 (2005)
- [23] M. W. C. Dharma-wardana and F. Perrot, *Phys. Rev. B*, **66**, 14110 (2002)
- [24] R. J. Elliott, J. A. Krumhansl, and P. L. Leath, *Rev. Mod. Phys.* **46**, 465 (1974)
- [25] Regarding the *VASP* code, see G. Kress, J. Furthmüller and J. Hafner, <http://cms.mpi.univie.ac.at/vasp/>
- [26] R. Ahlrichs, P. Scharf and K. Jankowski, *Chem. Phys.* **98**, 381(1985)
- [27] K. Iyakutti and M. W. C. Dharma-wardana, (unpublished)
- [28] M. W. C. Dharma-wardana (unpublished).
- [29] D. M. Ceperley and B. J. Alder, *Phys. Rev. Lett.*, **45**, 566 (1980); J. P. Perdew and A. Zunger, *Phys. Rev. B* **23**, 5043 (1981)
- [30] A. Altland, *Phys. Rev. Lett.* **97**, 236802 (2006)
- [31] N. M. R. Peres, F. Guinea and A. H. Castro Nito, [arXiv:cond-mat/0512091](https://arxiv.org/abs/cond-mat/0512091), and *Phys. Rev. B* **73**,125411 (2006)
- [32] N. H. Shon and T. Ando, *J. Phys. Soc. Jpn.* **67**,2421 (1998)
- [33] P. A. Lee, *Phys. Rev. Lett.* **71**, 1887 (1993)
- [34] M. W. C. Dharma-wardana, *Solid St. Com.* **140**, 4 (2006)
- [35] H. P. Dahal, Y. N. Jogleker, K. S. Bedall, and A. V. Blatsky *Phys. Rev. B* **74**, 233405 (2006)